Hybrid Solar Tower Pilot Plants for Co-Generation of Heat and Power for Brazilian Agro-Industry

Gilles Maag[1], Kimberly Tolentino de Oliveira[1], and Celso Eduardo Lins de Oliveira[1]

[1] University of São Paulo, Faculty of Zootechny and Food Engineering, Pirassununga, SP (Brazil).

Abstract

A currently undergoing project of two 100 kW_{el} central tower receiver concentrating solar power pilot plants for co-generation of heat and electricity for agro-industrial consumers is being presented. A strong agro-industrial sector and high solar resource make Brazil an ideal candidate for such a system. Grid-independent energy availability is ensured by hybrid firing of the plants' micro-turbines with bio-diesel. A steady-state-based model using DNI (Direct Normal Irradiance) values calculated from measured GHI (Global Horizontal Irradiance), using the DISC model, is applied to predict the yearly production of electricity of one of the plants and its degree of coverage of the associated slaughterhouse's requirements. An optical efficiency matrix of the heliostat field was obtained through ray-tracing simulations using the dedicated software tool Tonatiuh. Calculated yearly solar electricity production is 137 MWh, 76.5% of which can be used by the slaughterhouse, covering 48.5% of its consumption, the remainder being covered by bio-diesel. 23.5% of the produced solar electricity can be supplied to the grid. The yearly solar-to-electricity efficiency of the plant is 11.3%.

Keywords: c*o-generation, concentrated solar power, distributed generation, hybrid, solar tower, agro-industry, pilot plant.*

1. Introduction

CSP (Concentrating Solar Power) technology has been deemed a promising route for heat and power supply of agro-industrial processes in regions benefiting from high solar resource (> 2,000 $kWh \cdot m^{-2} \cdot y^{-1}$) as is the case for wide areas of Brazil, especially the North-East and Center regions. In regions of poor grid reliability and high electricity prices, CSP can be advantageous compared to other new renewable sources such as photovoltaics and wind power, by ensuring grid-independent energy availability thanks to thermal energy storage and hybridization with biofuels, and the possibility of co-generation of process heat. Previous studies considering implementation of solar energy applications in industry or agro-industry were able to individuate a significant potential for energy, process heat and cooling supply (Fuller, 2011; Mekhilef et al., 2011; Quijera et al., 2011a, 2011b; Tora et al., 2010).

To promote the use of CSP and demonstrating the functioning of the technology, the construction of two pilot-scale central tower receiver co-generation plants and their integration with agro-industrial facilities is currently undergoing in Pirassununga, São Paulo (case #1) and Caiçara do Rio do Vento, Rio Grande do Norte (case #2). Both plants use solar/bio-diesel hybrid-powered Brayton cycles, with 390 and 250 kW_{th} cavity receivers, respectively, operating with air at 1,173 K and 4.5 bar, powering 100 kW_{el} micro-turbines, as have been successfully operated and tested in past (Amsbeck et al., 2010). The solar field consists of 75 (case #1) and 47 (case #2) heliostats, each having a paraboloid-shaped, rectangular reflective surface of 8 m^2 area. A focal length of 30 m was chosen, close to the average distance to the receiver aperture (whose diameter is 0.9 m), situated at 25 m height. A design of the solar field and a process schematic are shown in Fig. 1.

doi:10.18086/swc.2015.04.22 Available at http://proceedings.ises.org

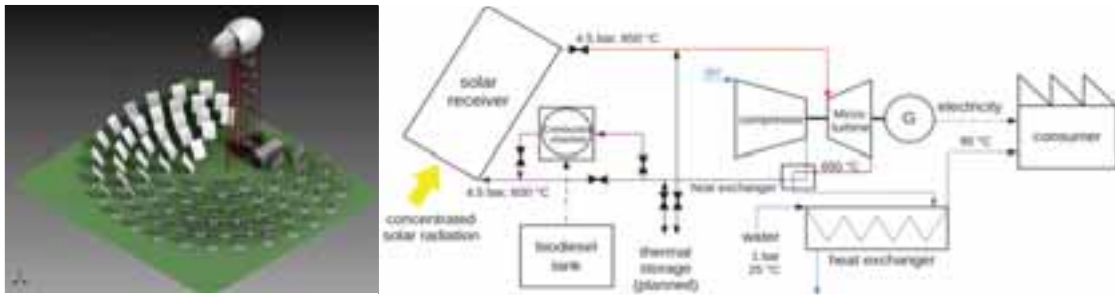

Fig. 1: Design of heliostat field for plant #1 (left), and process schematic of the two 100 kW_{el} hybrid solar tower plants (right).

Co-generation and tri-generation applications for microturbines (Buck and Friedmann, 2007; Ho et al., 2004; Kaikko and Backman, 2007), as well as solar turbine systems of various sizes and degrees of hybridization (Barigozzi et al., 2012; Le Roux et al., 2011; Schwarzbözl et al., 2006) have been proposed. The pilot plants are planned to provide energy and process heat supply to a school slaughterhouse (case #1) and a dairy factory (case #2). In this work, the performance of plant #1, in terms of electricity supply, is predicted using a numerical model based on 10 min steady-state intervals using DNI obtained from measured GHI data at the installation location.

2. Methodology

2.1. Solar resource

At the considered location (21°57' S, 47°26' W), only measured GHI data is available, in 10-min intervals, over a measurement period of 6 years. DNI values were estimated using the DISC model (Maxwell, 1987; Ineichen et al., 1992). From the individual data points, a probability distribution function f(DNI,m,h) is obtained for each discrete month m and hour h interval. Using a Monte Carlo numerical approach, the DNI at any time t is statistically determined using the following relationship:

$$\Re = \frac{\int_0^{\mathrm{DNI}(t)} F(\mathrm{DNI})|_{m,h} d\mathrm{DNI}}{\int_0^{\mathrm{DNI}_{\max}} F(\mathrm{DNI})|_{m,h} d\mathrm{DNI}} = \frac{\int_0^{\mathrm{DNI}(t)} F(\mathrm{DNI})|_{m,h} d\mathrm{DNI}}{1}, \quad \text{(eq. 1)}$$

with $F(\mathrm{DNI})|_{m,h}$ being the cumulative distribution function and$\Re$a random number [0;1[. The underlying assumption is that DNI values are statistically independent from those at previous times. This assumption, while differing from realistic conditions, is possible since steady-state conditions of the solar plant are assumed in each discretization interval (see Section 2.5.).

2.2. Solar resource

The radiative solar power incident on the heliostat field is then:

$$\dot{Q}_{\mathrm{field}}(t) = \mathrm{DNI}(t) A_{\mathrm{field}}, \quad \text{(eq. 2)}$$

with the reflective field area A_{field} = 602 m^2 and the radiative power entering the receiver cavity is:

$$\dot{Q}_{\mathrm{receiver,in}}(t) = \dot{Q}_{\mathrm{field}} \eta_{\mathrm{field}}\big(\alpha(t), \gamma(t)\big), \quad \text{(eq. 3)}$$

with $\alpha(t)$ and $\gamma(t)$ being the elevation and azimuth angle of the solar vector at time t, computed using the PSA Algorithm (Blanco-Muriel et al., 2001). A field efficiency matrix for 6 intervals $\Delta\alpha$ and 12 intervals $\Delta\gamma$ was computed using a collision-based Monte Carlo model of the heliostat field and the receiver aperture with the software Tonatiuh (Blanco et al., 2005). Linear interpolation was then used to determine $\eta_{\mathrm{field}}(\alpha,\gamma)$.

Net power absorbed by the receiver is:

$$\dot{Q}_{\mathrm{receiver,net}}(t) = \dot{Q}_{\mathrm{receiver,in}} - \dot{Q}_{\mathrm{reradiation}} - \dot{Q}_{\mathrm{conduction}}, \quad \text{(eq. 4)}$$

with

$$\dot{Q}_{\mathrm{reradiation}}(t) = \varepsilon \sigma T^4, \quad \text{(eq. 5)}$$

where T is the receiver temperature. Assuming the receiver efficiency

$$\eta_{\text{receiver}}(t) = \frac{\dot{Q}_{\text{receiver,net}}(t)}{\dot{Q}_{\text{receiver,in}}(t)}, \quad \text{(eq. 6)}$$

to be 90% at nominal operation point (21st December, solar noon, DNI = 1,000 W m^{-2}, denoted by subscript "N") allows to calculate $\dot{Q}_{\text{receiver,net,N}}$ at the same point using Eq. 6. If constant receiver temperature T = 1,173 K, and ambient temperature T_∞ = 298 K are assumed, $\dot{Q}_{\text{conduction}}$ and $\dot{Q}_{\text{reradiation}}$ are constant and can be determined using Eqs. 4 and 5 at nominal operation point. $\dot{Q}_{\text{receiver,net}}(t)$ can then be calculated at every time by Eq. 4. If the combined losses are higher than $\dot{Q}_{\text{receiver,in}}(t)$, receiver operation is stopped. Similarly, an upper threshold of $\dot{Q}_{\text{receiver,in,max}} = 1.05\dot{Q}_{\text{receiver,in,N}}$ is defined.

2.3. Consumer requirements

Based on their 2013 production and typical electricity consumption values per amount of produced meat, the consumer's yearly electricity consumption $W_{\text{consumer,}}$ is estimated to be 215 MWh$_{\text{el}}$. Assuming 30% of this value being for refrigeration (operated 24 hours-a-day) and 70% for plant operation during working hours (9 hours-a-day, 8am – 5pm), the following consumer power consumption is determined:

$$P_{\text{consumer}}(t) = \begin{Bmatrix} 54.4\ \text{kW}_{\text{el}}, \text{8am - 5pm} \\ 6.8\ \text{kW}_{\text{el}}, \text{5pm - 8am} \end{Bmatrix}. \quad \text{(eq. 7)}$$

2.4. Power block

No thermal losses are assumed between receiver and microturbine. The microturbine is assumed to have a constant thermal efficiency etaturbine = 0.28. Electrical power produced from solar source is then:

$$P_{\text{solar}}(t) = \dot{Q}_{\text{receiver,net}}\eta_{\text{turbine}}. \quad \text{(eq. 8)}$$

If the solar resource is insufficient to cover the consumer's requirement, the remainder is delivered by biofuel:

$$P_{\text{biofuel}}(t) = \begin{Bmatrix} P_{\text{consumer}}(t) - P_{\text{solar}}(t), \text{for: } P_{\text{consumer}}(t) \geq P_{\text{solar}}(t) \\ 0\ \text{kW}_{\text{el}}, \text{for: } P_{\text{consumer}}(t) < P_{\text{solar}}(t) \end{Bmatrix}. \quad \text{(eq. 9)}$$

On the other hand, if the solar resource exceeds the consumer's needs, and the legislative framework allows for it, solar electricity can be supplied to the grid:

$$P_{\text{grid}}(t) = \begin{Bmatrix} P_{\text{solar}}(t) - P_{\text{consumer}}(t), \text{for: } P_{\text{solar}}(t) \geq P_{\text{consumer}}(t) \\ 0\ \text{kW}_{\text{el}}, \text{for: } P_{\text{solar}}(t) < P_{\text{consumer}}(t) \end{Bmatrix}. \quad \text{(eq. 10)}$$

The field efficiency, reactor efficiency, and total plant efficiency are obtained as follows:

$$\eta_{\text{field}}(t) = \frac{\dot{Q}_{\text{receiver,in}}(t)}{\dot{Q}_{\text{field}}(t)}, \eta_{\text{receiver}}(t) = \frac{\dot{Q}_{\text{receiver,net}}(t)}{\dot{Q}_{\text{receiver,in}}(t)}, \eta_{\text{plant}}(t) = \frac{P_{\text{solar}}(t)}{\dot{Q}_{\text{field}}(t)}. \quad \text{(eq. 11)}$$

The solar fraction of total produced electrical energy, the solar fraction of the slaughterhouse's consumption, and the fraction of solar electricity delivered to the grid are defined as:

$$\varphi_{\text{solar}}(t) = \frac{W_{\text{solar}}(t)}{W_{\text{biofuel}}(t)+W_{\text{solar}}(t)}, \ \varphi_{\text{consumer,solar}}(t) = \frac{W_{\text{solar}}(t)-W_{\text{grid}}(t)}{W_{\text{consumer}}(t)}, \ \varphi_{\text{solar,grid}}(t) = \frac{W_{\text{grid}}(t)}{W_{\text{solar}}(t)}. \quad \text{(eq. 12)}$$

2.5. Yearly/monthly performance and discretization

Heat energy consumed Q or generated electrical work W over a given time lapse $t_0 \leq t \leq t_f$ – here: one month or one year - is obtained by integration. A numerical solution is obtained by discretization in time intervals Δt = 600 s, over which time-dependent variables are assumed to be constant.

$$\{Q, W\} = \int_{t_0}^{t_f}\{\dot{Q}(t), P(t)\}dt \approx \sum_{i=1}^{(t_f-t_0)/\Delta t}\{\dot{Q}_i, P_i\}\,\Delta t. \quad \text{(eq. 13)}$$

Finally, the capacity factors of the solar plant and of the power block are:

$$c_{\text{solar}} = \frac{W_{\text{solar}}}{P_{\text{solar,N}}(t_f-t_0)}, \ c_{\text{power block}} = \frac{W_{\text{solar}}+W_{\text{biofuel}}}{(P_{\text{solar,N}}+P_{\text{biofuel,N}})(t_f-t_0)}. \quad \text{(eq. 14)}$$

3. Results

Figure 2 shows the electrical power generation from solar source and the consumer's consumptions for three different selected examples of day: (a) on 21st December, with DNI(t) > $DNI_{85\%}$, (b) on 21st March, with DNI(t) varying over the entire statistical distribution, and (c) on 21st June, with DNI(t) < $DNI_{30\%}$. In is shown that for days with very good solar resource, the entire daytime consumption of the slaughterhouse can be supplied by solar energy.

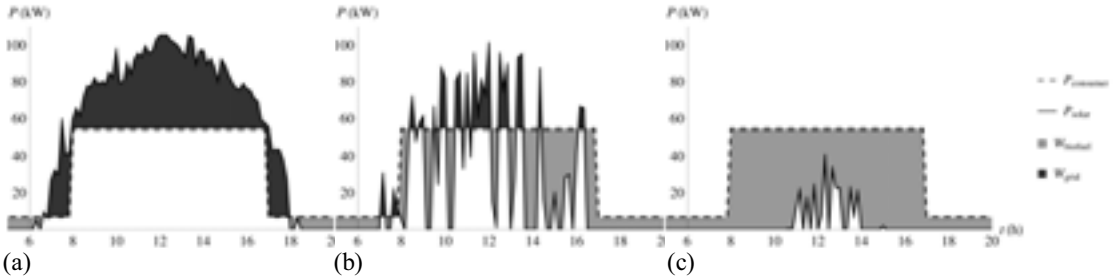

(a) (b) (c)

Fig. 2: Electricity generation from solar source and consumption by the slaughterhouse for: (a) Dec. 21st, DNI(t) > $DNI_{85\%}$; (b) Mar. 21st; (c) Jun. 21st, DNI(t) < $DNI_{30\%}$.

However, for less sunny days, such as case (b) or (c), significant amounts of biofuel are needed to supply the required electricity. Especially in case (b), the addition of TES (Thermal Energy Storage) could significantly decrease this amount.

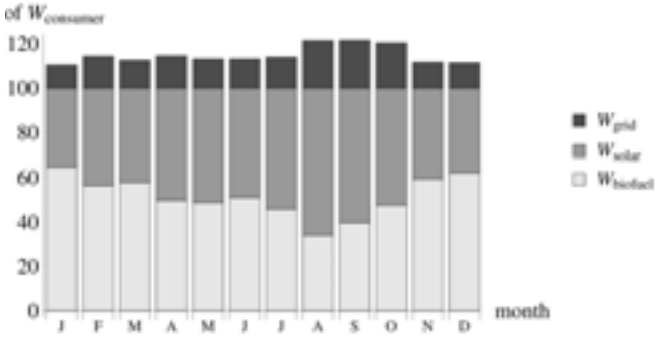

Fig. 3: Monthly source and utilization distribution of generated electricity in % of $W_{consumer}$.

This solar fraction is shown in Fig. 3 for each month, which shows the totally generated electrical energy per source and destination, as a percentage of total consumption by the slaughterhouse. The solar fraction of the slaughterhouse varies between 35.2% in January and 65.9% in August, with a yearly value of 48.5%. These relatively high solar fractions are favored by the hourly distribution of the consumer's consumption, which is significantly higher during daytime. The solar fraction of total electricity generated lies between January's 41.4% and August's 71.9%. The yearly average is 55.2%. These values are higher, since a yearly average of 23.5% of solar energy is supplied to the grid, since it exceeds the consumption. The addition of a TES system would allow to reduce the biofuel consumption, currently at 44,360 l y^{-1}, if bio-diesel (LHV = 32.3 MJ l^{-1}) were to be employed. The present analysis does not assume biofuel-generated electricity to be supplied to the grid. Depending on the biofuel type/cost and electricity market prices, this may however be the case.

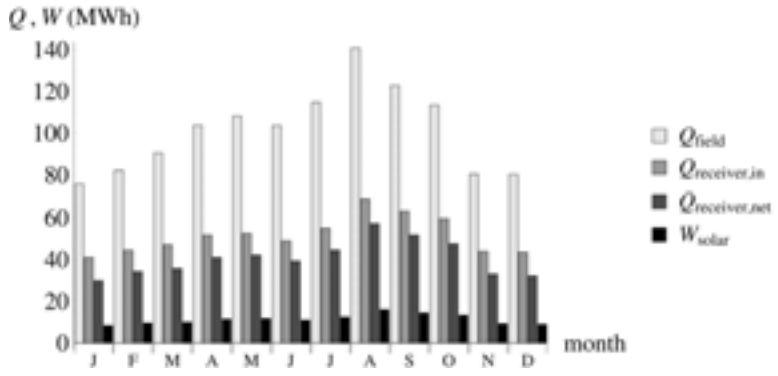

Fig. 4: Monthly energetic performance of solar plant.

Figure 4 shows the performance of the solar plant in terms of field, receiver, and power block energy losses. The solar-to-electrical energy efficiency of the plant is slightly varying seasonally (10.7% - 11.8%) due to differences in field efficiency. The yearly value is 11.3%. While this value is relatively low, also due to the small size and pilot nature of this plant, the total efficiency of the plant can be significantly improved by co-generation of power and heat, which will be done for this plant, but an analysis of which is out of the scope of this work. From both Fig. 3 and 4 it is observable that, due to the tropical location of the plant, the influence of astronomical factors (length of day, sun elevation) on plant performance is superseded by that of seasonal atmospheric phenomena (such as dry/wet period), resulting in poor summer performance, compared to late winter/early spring.

Tab. 1: Summary of nominal (on Dec. 21, solar noon, DNI_N = 1,000 W m^{-2}) and yearly plant parameters.

Nominal parameters			Yearly parameters		
$\dot{Q}_{\text{field,N}}$	kW	602.0	Q_{field}	MWh	1,216.5
$\dot{Q}_{\text{receiver,in,N}}$	kW	397.0	$Q_{\text{receiver,in}}$	MWh	621.0
$\dot{Q}_{\text{receiver,net,N}}$	kW	357.2	$Q_{\text{receiver,net}}$	MWh	489.9
$P_{\text{solar,N}}$	kW_{el}	100.0	W_{solar}	MWh_{el}	137.2
$P_{\text{biofuel,N}}$	kW_{el}	0.0	W_{biofuel}	MWh_{el}	111.3
$P_{\text{grid,N}}$	kW_{el}	45.6	W_{grid}	MWh_{el}	32.3
$\dot{V}_{\text{biofuel}}$	l/h	0.0	V_{biofuel}	l	44,360*
$\eta_{\text{field,N}}$		0.659	η_{field}		0.510
$\eta_{\text{receiver,N}}$		0.900	η_{receiver}		0.789
$\eta_{\text{turbine,N}}$		0.280	η_{turbine}		0.280
$\eta_{\text{plant,N}}$		0.166	η_{plant}		0.28
$\varphi_{\text{solar,N}}$		1.000	φ_{solar}		0.552
$\varphi_{\text{consumer,solar,N}}$		1.000	$\varphi_{\text{consumer,solar}}$		0.485
$\varphi_{\text{solar,grid,N}}$		0.456	$\varphi_{\text{solar,grid}}$		0.235
			c_{solar}		0.157
			$c_{\text{power block}}$		0.284
*if bio-diesel (LHV = 32.3 MJ l-1) is used.					

A summary of the nominal and principal yearly parameters of the plant can be found in Tab. 1.

4. Conclusions

A steady-state-based numerical model for the prediction of a solar/biofuel hybrid central tower receiver power plant was formulated and used to simulate the performance of a 100 kW_{el} pilot plant to be built in Pirassununga, São Paulo, Brazil, to deliver electricity and heat to a slaughterhouse. The results show a yearly generation potential of 137.1 MWh_{el} from solar energy. A yearly average of 76.5% of the produced solar electricity can be used by the slaughterhouse, covering 48.5% of its consumption. The remainder is covered by bio-diesel (44,360 l y^{-1}). The remaining 23.5% of the produced solar energy can be sold to the grid. Alternatively, TES would allow to postpone the generation of this energy fraction, allowing for a reduction in bio-fuel consumption. The energy balance of the solar plant shows a total plant efficiency of 11.3%. An influence of dry/wet season on the plant performance is observed, as opposed to the typical summer/winter effect generally observed at higher-latitude locations.

Acknowledgements

The authors thank Lars Amsbeck and Andres Pfahl (DLR) for the dimensioning and design of the heliostat field and Maicon D. Bastos for the slaughterhouse consumption data. The image of the planned solar plant is courtesy of Rafael Gonsales Neto (Solinova, Ltda.). The SMILE (Solar-hybrid Micro-turbine Systems for Co-generation in Agro-industrial Electricity and Heat Production) project is funded by BNDES (under the FUNTEC financing line), Elektro (Eletricidade e Serviços) S/A, and Solinova, Ltda.

Nomenclature

A	area, m^2
c	capacity factor
F	cumulative probability distribution function
f	probability distribution function
h	discrete hour interval
m	discrete month interval
P	Electric power, W
Q	Thermal energy, kWh
$\dot{Q}$	Thermal power, W
T	Temperature, K
t	time, s
W	Electric energy/work, kWh

Greek letters

α	Elevation angle of solar vector, °
γ	Azimuth angle of solar vector, °
ε	Surface emissivity
η	Energy conversion efficiency
σ	Stefan-Boltzmann constant, 5.6703 10^{-8} W m^{-2} K^{-4}
φ	fraction

Other symbols

$\Re$	pseudo-random number [0;1[

Subscripts

0	initial
x%	x^{th} percentile

el	electric
f	final
field	heliostat field
N	nominal
receiver,in	incident on receiver aperture
receiver,net	Net absorbed by receiver

Abbreviations

DNI	direct normal irradiance, W m^{-2}
GHI	global horizontal irradiance, W m^{-2}
LHV	lower heating value, MJ kg^{-1}
TES	thermal energy storage

References

Amsbeck, L., et al. 2010. Test of a solar-hybrid microturbine system and evaluation of storage deployment, in: Proceedings of SolarPACES 2010 Conference, Perpignan, France, September 21-24, 2010.

Barigozzi, G., et al., 2012. Thermal performance prediction of a solar hybrid gas turbine. Sol. Energ. 86, 2116-2127.

Blanco, M., et al., 2005. The Tonatiuh Software Development Project: An Open Source Approach to the Simulation of Solar Concentrating Systems. In: Proceedings of the ASME 2005 International Mechanical Engineering Congress and Exposition, Orlando, FL, USA, November 5-11, 2005.

Blanco-Muriel, M., et al., 2001. Computing the solar vector. Sol. Energ. 70, 431-441.

Buck, R., Friedmann, S., 2007. Solar-Assisted Small Solar Tower Trigeneration Systems, J Sol. Energ. Eng. 129, 349-354.

Fuller, R.J., 2011. Solar industrial process heating in Australia - Past and current status. Renewable Energ. 36, 216-221.

Ho, J.C., Chua, K.J., and Chou S.K., 2004. Performance study of a microturbine system for cogeneration application. Renewable Energ. 29, 1121-1133.

Ineichen, P., et al., 1992. Dynamic global-to-direct irradiance conversion models. ASHRAE Transactions 98, 354-369

Kaikko, J., Backman, J., 2007. Technical and economic performance analysis for a microturbine in combined heat and power generation. Energy 32, 378-387.

Le Roux, W.G., Bello-Ochende, T., Meyer J.P., 2011. Operating conditions of an open and direct solar thermal Brayton cycle with optimized cavity receiver and recuperator. Energy 36, 6027-6036.

Maxwell, E.L., 1987. A Quasi-Physical Model for Converting Hourly Global Horizontal to Direct Normal Insolation. SERI Technical Report SERI/TR-215-3087.

Mekhilef, S., et al., 2011. A review on solar energy use in industries. Renewable Sustainable Energ. Review 15, 1777-1790.

Quijera, J.A., et al., (2011) Integration of a Solar Thermal System in a Dairy Process. Renewable Energ. 36, 1843-1853.

Quijera, J.A., et al., (2011) Usage of solar energy in industrial process. Chem. Eng. Transactions 25, 875-880.

Schwarzbözl, P., et al. (2006) Solar gas turbine systems: Design, cost, and perspectives. Solar Energ. 80, 1231-1240.

Tora, E.A., El-Halwa, M.M. (2010), Integration of Solar Energy into Absorption Refrigerators and Industrial Processes. Chem. Eng. Technol. 9, 1495-1505.